Available online at www.sciencedirect.com
SCIENCE DIRECT®
Optical Materials 27 (2005) 1305–1310
OPTICAL Materials
www.elsevier.com/locate/optmat

Enhanced cooperative absorption and upconversion in Yb^{3+}doped YAG nanophosphors

L.A. Diaz-Torres [a,*], E. De la Rosa [a], P. Salas [b], H. Desirena [a]

[a] *Centro de Investigaciones en Optica A.C., Leon, Gto. 37150, Mexico*
[b] *Instituto Mexicano del Petroleo, D.F., 07730, Mexico*

Received 4 October 2004; accepted 20 October 2004
Available online 18 January 2005

Abstract

Enhanced cooperative absorption and upconversion emission of Yb^{3+} pairs in nanocrystalline YAG is observed. The nanocrystallites synthesized by a modified sol–gel method have an average size of 96 nm. The estimated concentration normalized ratio of maximum visible absorption to maximum IR absorption emission of 7.55×10^{-22} cm^3 is about four orders of magnitude higher than the highest reported value to date, and more than seven orders higher than for bulk monocrystalline YAG:Yb^{3+}. Strong cooperative upconversion emission is observed under IR pump at 940 nm.

Keywords: Cooperative absorption; Upconversion; Yb^{3+}; Nanophosphors

1. Introduction

The upconversion (UC) of low-energy photons to high-energy photons is a well-studied phenomenon that now has use in many applications. These include solid-state lasers, phosphor materials, optical data storage, IR counters, among other devices which have the advantage of cheap and readily available excitation sources, namely IR diodes, as well as consisting of all solid-state components. A broad group of new UC phosphors emitting in the visible range share an important characteristic: they are sensitized with Yb^{3+} [1–3]. The special electronic configuration of Yb^{3+} makes the 4f electrons less shielded than in other ions of the lanthanide series, showing a higher tendency to interact with the lattice and neighbor ions. These characteristics make Yb^{3+} an excellent sensitizer for most of the rare earth (RE) and transition metals (TM) ions, where the main energy transfer mechanism is the so called cooperative UC process, first proposed by Ovsyankin and Feofilov [4]. On such proposal two excited Yb^{3+} ions transfer their electronic excitation energy simultaneously to a nearby RE (or TM) ion, which subsequently emits a photon with the sum of energies, plus (or minus) y slight amount due to phonon coupling. Such process has been observed even when there are only Yb^{3+} ions in the host [5–8]. That is, when there is neither an intermediate nor a final energy level (from the codopant) to be populated in order to emit in the visible. Such cooperative UC (CUC) was first observed by Nakazawa in $YbPO_4$ [9]. In most of the cases such CUC phenomena is accompanied by cooperative absorption [5,10], optical bistability [7], and splitting of the ground and excited states [1,7]. Cooperative UC, cooperative absorption and bistability have been observed in several monocrystalline Yb^{3+} doped yttrium oxides [5,7]. In particular it has been observed in YAG planar waveguides [5]. However, for bulk YAG neither the emission nor the absorption processes are strong enough to be quantified

* Corresponding author.
E-mail address: ditlacio@cio.mx (L.A. Diaz-Torres).

0925-3467/$ - see front matter © 2004 Elsevier B.V. All rights reserved.
doi:10.1016/j.optmat.2004.10.020

in a proper way [7]. That has ruled out monocrystalline YAG as a good candidate for RE and TM emission applications based on the above cooperative processes.

On the other side, the use of polycrystalline ceramics as a new type of laser gain host has been intensively investigated because they have several advantages over single-crystal hosts [11–13]. For example, ceramic samples with a high doping concentration and a large size can be easily fabricated, whereas this is extremely difficult for single crystals: multiplayer and multifunctional ceramic laser materials are possible because of the polycrystalline nature of ceramics. Potentially, because of the short period of fabrication process and because they can be mass-produced, the cost of ceramic laser materials could be much lower than that of single crystals. In particular, no complicated facilities and critical techniques are required for growth of ceramics. The most important condition to fabricate ceramics is that the starting polycrystalline powders have a nanosized character with a uniform distribution of particles. Driven by these advantages, excellent quality Nd^{3+} doped ceramic laser materials have been developed that are a good alternative to the widely used Nd:YAG single crystals [14]. Besides Nd^{3+} doped ceramic laser materials, there has been a growing interest in trivalent ytterbium-doped ceramics. Compared with Nd^{3+} doped ceramics, Yb^{3+} doped ceramic laser materials are more attractive for ultrashort pulse lasers because of their broad absorption and emission bandwidths [15]. As a new type of Yb^{3+} doped laser material, Yb:Y_2O_3 ceramic has been experimentally demonstrated to be a promising diode-pumped laser medium [14]. Recently, nanocrystalline pure and RE doped YAG has been synthesized by a modified sol–gel method [16]. The luminescent and termoluminescent properties of these nanocrystals have shown to be more promising that the ones from their monocrystalline counterparts.

In the present work we searched for the cooperative absorption and emission in Yb^{3+} doped nanocrystalline YAG (NCYAG). By comparing its cooperative characteristics against the reported literature for monocrystalline YAG, as well as other oxides, it has been found a considerable enhancement of the cooperative processes, showing better performance than the most efficient Yb^{3+} doped oxide reported to date: Sc_2O_3:Yb^{3+} [7].

2. Experimental procedure and discussion

2.1. Synthesis of NCYAG

The nanocrystalline YAG (NCYAG) samples were prepared by a modified sol–gel method [16] and the schematic diagram of the process is shown in Fig. 1. All chemicals were reactive grade and supplied by Aldrich, Inc. In a first baker (b1), yttrium nitrate ($Y(NO_3)_3$–$5H_2O$) was dissolved with 100 ml of CO_2-free distilled water, previously mixed with 2 ml of acetic acid (CH_3CO_2H) by stirring the mixture for 2 h at 50 °C. In a second baker (b2), the aluminium nitrate ($Al(NO_3)_3$–$9H_2O$) was dissolved in 50 ml of CO_2-free distilled water by stirring for 1 h at room temperature. Ytterbium samples were prepared adding to the aluminium solution the corresponding quantity of impurity salts for 5 mol% of ytterbium oxide. Then, both solutions were mixed and complexed with 2 ml of 1,2-ethanediol (ethylene glycol) and stirred again until obtain a homogeneous and transparent solution. The resulting solution was stirred at 70 °C to evaporate slowly all the solvents until foam was formed. The foam was dried at 120 °C and then grinded in an agate mortar to obtain a fine powder. These powder Samples were annealed at 700 °C for 6 h and then the temperature was raised to 900 °C for 12 h using a 5 °C/min temperature rate. Finally, the temperature was increased to 1150 °C and kept there for 4 h.

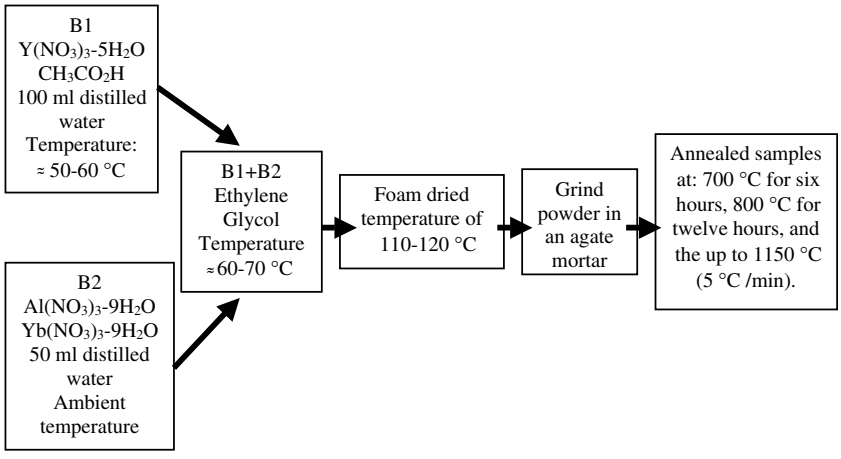

Fig. 1. Schematic diagram of the steps for the synthesis method.

2.2. Structural and morphological characterization

The crystalline structure of the nanophosphor was characterized by X-ray diffraction (XRD) using a Siemens D-500 equipment with Cu Kα radiation at 1.5426 Å. The spectra for were obtained from 4° to 70° with increments of 0.03° and a swept time of 0.6 s. Fig. 2 shows the XRD patterns for the NCYAG:Yb (5%). All the XRD peaks were indexed in terms of the garnet structure according to the standard JCPDS # 33-0040. The main peak of the cubic YAG structure is at $2\theta = 33.5°$, and corresponds to the crystalline plane with Miller indices (4,2,0). No secondary impurity phase such as $Y_4Al_{12}O_9$ (YAM), $YAlO_3$ (YAP), Yb_2O_3, or Y_2O_3 was observed. The average crystallite sizes were calculated by using the Scherrer's equation [17]:

$$D = (0.9\lambda)/\beta\cos(\theta). \quad (1)$$

Here, λ is the X-ray wavelength, β is the corrected half-width of the strongest diffraction peak and θ is the diffraction angle. The crystallite size for the samples was 96 nm with no observable dependence on the Yb3+ concentration. Transmission electron microscopy (TEM) images were taken on a JEOL JEM-2010FEG microscope operating at an accelerating voltage of 200 kV, see inset in Fig. 2. Powder samples were suspended in isopropanol and the aliquots were dropped on 3 mm diameter Lacey Carbon cooper grids. The TEM image shows clearly each individual nanocrystals that compose the observed microparticle. Also, it can be observed that the crystallite size agrees well with the values obtained by X-ray diffraction. Notice the great uniformity of the average nanocrystallite size around 96 nm.

2.3. Absorption and photoluminescence

The optical absorption spectra (reflectance mode) were measured with a Perkin–Elmer UV-VIS-NIR Lambda 900 by using a 1.5 in. integrating sphere (Labsphere Co.). Photoluminescence spectra were measured with a conventional set-up, the sample was placed in a mobile holder to be aligned. Excitation at λ exc = 940 nm from an Optical Parametric Oscillator (Quanta Ray, MOPO-730 pumped with a Q-switched Nd:YAG laser Quanta Ray, GCR230-10) was used. The emission was collected at 45° from the pumping signal and focused on the slit entrance of a 0.5 m Acton Research monochromator to obtain the spectra with a resolution of 0.1 nm. Appropriated VIS and IR PMTs were coupled to the exit slits of the monochromator and their signal sent to a Stanford Research lock in amplifier. The output signal was stored and plotted in a computer. For lifetime measurements the same set up was used but the corresponding PMT signal was send to a 500 MHz oscilloscope with a coupling of 50 Ω and triggered by the excitation laser trigger. All measurements were done at room temperature.

Single Yb^{3+} ions have (only) two stark-split energy manifolds, the ground state $^2F_{7/2}$ and the excited state $^2F_{5/2}$ around 10,000 cm^{-1}. Cooperative absorption and emission occurs in the visible range of the spectrum, between 19,000 and 23,000 cm^{-1} [3–10]. Fig. 3, shows the absorption spectra for the NCYAG:Yb (5%) sample. Curve (a), corresponding to the IR, has been scaled by a factor of (1/1.879) to make it comparable with the VIS cooperative absorption band shown in curve (b). The observed IR absorption band is in agreement with the previous reported spectra for Yb^{3+} in YAG [5,18]. It is also observed that the cooperative absorption spectra is in well agreement with the self-convolution, $\int f_{IR}(v) f_{IR}(E-v)\,dv$, of the IR absorption, $f_{IR}(v)$, depicted by curve (c) [3,7,8]. This is the best evidence that the observed visible band spectra were in fact due to simultaneous cooperative absorption of paired Yb^{3+} ions. It is noticeable that no other detectable lines or bands corresponding to trace impurities of other R.E. (or TM) ions were observed in the visible region.

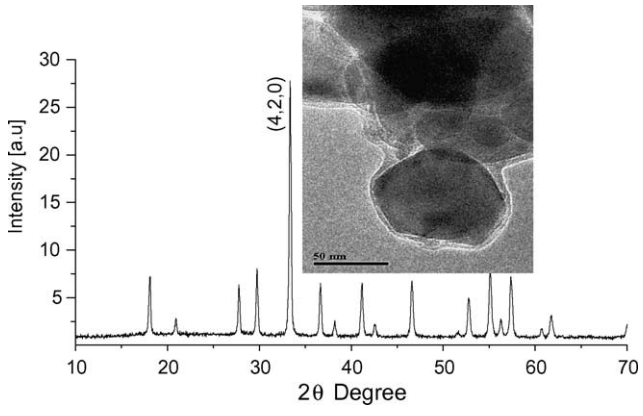

Fig. 2. XRD spectrum of the NCYAG:Yb (5%) sample annealed at 1150 °C, and TEM micrograph of the same sample.

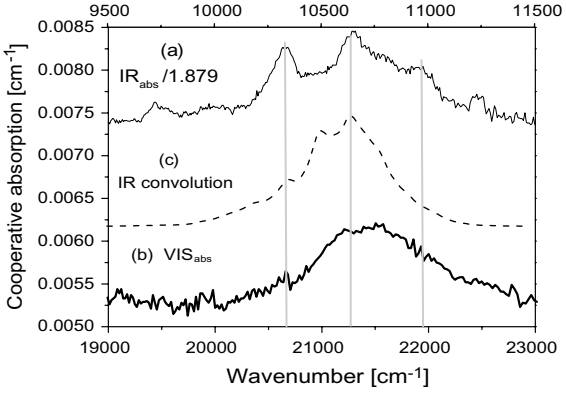

Fig. 3. IR absorption of Yb^{3+} ions in NCYAG:Yb (5%), (a), cooperative absorption of Yb^{3+} pairs, (b), and self-convolution of the IR absorption spectrum, (c).

Reported data on the position of the stark energy levels of Yb^{3+} in YAG are contradictory [19,20], that mainly due to the wide band structure of the absorption spectra itself. That avoids to theoretically predicting, by a discrete convolution, the probable positions for the cooperative Yb^{3+} pair absorption lines. However, from Fig. 3, its is likely that the visible absorption peaks and shoulder at 20,661, 21,276, and 21,929 cm^{-1} correspond to the doubled energy of the principal IR absorption peaks at 10,335 cm^{-1} (967.58 nm), 10,638 cm^{-1} (940.02 nm), and 10,970 cm^{-1} (911.52 nm), respectively. One can also observe that the two first are in concordance with the corresponding peaks on the self-convolution of the IR spectrum.

In Ref. [7] it is reported the dependence of the ratio of the maximum visible absorption intensity to the maximum IR absorption intensity (at $0 \rightarrow 0$ transition), normalized to the concentration of Yb^{3+} ions, $\eta_{coop}^{abs} = (k_{VIS}^{abs}/k_{VIS}^{abs}N_{Yb}) = (\sigma_{VIS}/\sigma_{IR})$, versus the minimum Yb–Yb distance, r_{min}. There, it is shown that the highest value for η_{coop}^{abs}, 1.5×10^{-26} cm^3, corresponds as expected to the monocrystal with the shortest $r_{min}^{Sc_2O_3} = 3.27$ Å. That is, the Sc_2O_3 monocrystal possesses the most efficient cooperative absorption. It is worth to notice that in Table 1 of Ref. [7] there is no reported value for monocrystalline YAG:Yb(10%) since the cooperative absorption was not measurable. Further more, the cooperative emission was rather difficult to observe and not measurable with the available experimental setup. That is in agreement with the expected behavior, that as r_{min} increases then η_{coop}^{abs} decreases with a power dependence of $(r_{min})^{-6}$ [7], because $(r_{min}^{YAG} = 3.67\ Å) > (r_{min}^{Yb_3Al_5O_{12}} = 3.65\ Å) > r_{min}^{Sc_2O_3}$, and $\eta_{coop}^{abs} = 3.9 \times 10^{-28}$ cm^3 for $Yb_3Al_5O_{12}$ is two orders of magnitude smaller than for Sc_2O_3:Yb(6%). Therefore, the expected value of η_{coop}^{abs} for monocrystalline YAG:Yb (5%) has to be smaller than 3.9×10^{-28} cm^3. However, from the spectra shown in Fig. 3 for NCYAG:Yb (5%) it is estimated a value of

$$\eta_{coop}^{abs} = \left(\frac{k_{VIS}^{abs}}{k_{IR}^{abs}N_{Yb}}\right) = \left(\frac{0.00621}{0.01175 * 0.07 \times 10^{22}\ cm^{-3}}\right) = 7.55 \times 10^{-22}\ cm^3. \quad (2)$$

This value is about four orders of magnitude higher than for Sc_2O_3:Yb(6%), and was not expected since $(r_{min}^{NCYAG:Yb\ (5\%)} = 3.668\ Å) > r_{min}^{Sc_2O_3}$. The value for $r_{min}^{NCYAG:Yb\ (5\%)}$ was estimated by scaling the lattice parameters of YAG (12.011 Å) to the lattice parameters for NCYAG:Yb (5%) (12.004 Å, estimated from the XRD spectra in Fig. 2). Such an anomalous value of η_{coop}^{abs} could be explained by considering the suggestion that in nanocrystalline oxide ceramics the RE impurity ions diffuse to the outer part of the nanocrystallite [21]. Then, there is a gradient of Yb^{3+} concentration from the center to the surface of the nanocrystallite. That gradient will promote a higher concentration of Yb^{3+} pairs at the distorted lattices near the surface. In addition, such outer lattice cells will have shorter minimum distances due to surface reconstruction of the crystallites and higher Yb^{3+} concentrations. Therefore, the overall result is a higher effective concentration of Yb^{3+} pairs at the nanocrystallite surface with $r_{min}^{Yb\ pairs} < r_{min}^{NCYAG:Yb\ (5\%)}$. Thus, the nanosized nature of the NCYAG:Yb (5%) phosphors allows an enhanced cooperative absorption in comparison with the single ion IR absorption from Yb^{3+} ions in the center of the nanocrystallite or far enough of other Yb^{3+} ions to form cooperative pairs.

As cited above CUC emission from Yb^{3+} pairs in bulk YAG has been rather difficult to observe [7], most of the reported literature about YAG:Yb only considers the IR emission since the cooperative emission is negligible. There is only one previous work to our knowledge that observed and quantified the CUC emission of bulk YAG:Yb^{3+} in 24 μm thick planar epitaxial waveguides [5]. In that work it is shown that the cooperative emission in the waveguide is about twice the cooperative emission in bulk YAG. It is also concluded that such an efficient cooperative emission might be due to ion clustering within the waveguide. Fig. 4 shows the room temperature IR and CUC emissions form NCYAG:Yb (5%), curves (a) and (b), respectively, under pumping at 940 nm (10,638.29 cm^{-1}). The IR emission agrees well with the reported data [7,18,19,21] for bulk YAG:Yb^{3+}, having the two main characteristic peaks at 9689 cm^{-1} (1032 nm) and 10,303.967 cm^{-1} (970.5 nm). Also, the self-convolution of the IR emission is shown in curve (c). The self-convolution has four main peaks at 19,038, 19,398, 19,997, and 20,596 cm^{-1}. One can note that the second and fourth peaks correspond to the doubled energy peaks of the IR emission. The CUC emis-

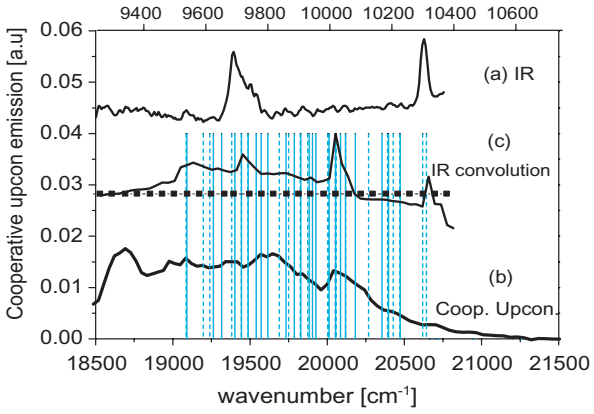

Fig. 4. IR emission of Yb^{3+} ions in NCYAG:Yb (5%), (a), cooperative emission of Yb^{3+} pairs, (b), and self-convolution of the IR emission spectrum, (c). Light gray vertical lines indicate the theoretically expected positions for cooperative emission peaks.

sion, curve (b), has a fair correspondence with the self-convolution of the IR emission, at least the first three peaks of the convolution can be distinguished in the cooperative emission. The last one could be assigned to a small shoulder in the cooperative emission at 20,596 cm^{-1}. In addition, on Fig. 4 are shown a series of lines that mark the theoretically expected lines for cooperative emission on YAG:Yb^{3+} [5,7]. The great number of such possible emission lines explains why the cooperative emission presents smooth and wide bands. That is the case for the observed band from 18,800 to 21,500 cm^{-1}.

There is also the possibility to observe unwanted impurity RE emission lines together with the cooperative ones for wavenumbers higher than 19,800 cm^{-1}, being the more important the one from Tm^{3+} ions at 20,600 cm^{-1}, and for wavenumbers lower than 18,800 cm^{-1}, from Er^{3+} and Ho^{3+}. In fact, we only observe Er^{3+} emission lines at 18,691 cm^{-1} (shown in Fig. 4) and below corresponding to the green and red emissions of Er^{3+} (not shown in Fig. 4). The most intense of such bands is the green band and is about three times more intense than the cooperative emission. That is a curious result since the amount of Er^{3+} impurities has to be quite low, certainly it was not possible to detect its presence in the absorption measurements and our starting compounds were 5 N graded. On the other side, this intense Er^{3+} emission indicates that there is a very efficient UC process involving the trace Er^{3+} ions and having the Yb^{3+} ions as sensitizers. An explanation to that phenomenon is given by considering CUC among Yb^{3+} pairs and Er^{3+} single ions. Of course, such Er^{3+} CUC is deleterious to the Yb^{3+} pair cooperative emission. One interesting thing to notice is that YAG is the only yttrium system were trace impurities become important when observing the Yb^{3+} emission.

The above results confirm that the lattice distortion of superficial lattice cells, due to the nanosized character of NCYAG:Yb (5%), and the diffusion of RE ions to the surface of the nanocrystallites promote strong first neighbors interactions, due to an increased relative concentration of RE ions and reduced minimum distances among RE ions near the surface of the nanocrystallite. Such very strong cooperative interactions could explain how it is possible to observe strong emission coming out from trace concentrations of Er^{3+} when pumping a nominal Yb^{3+} concentration. Being the trace emission stronger than the emission from the nominal dopant, Yb^{3+} in this case. Further work is in progress to investigate the effects of the variation of the crystallite size on the cooperative processes in NCYAG:Yb^{3+}.

The luminescence decay times, at room temperature, of both the VIS CUC emission and the IR $^2F_{5/2}$ manifold emission were investigated and the results produced time constants of 1.35 ms at 1032 nm and 0.5 ms at 516 nm, respectively, as illustrated in Fig. 5. Both decays

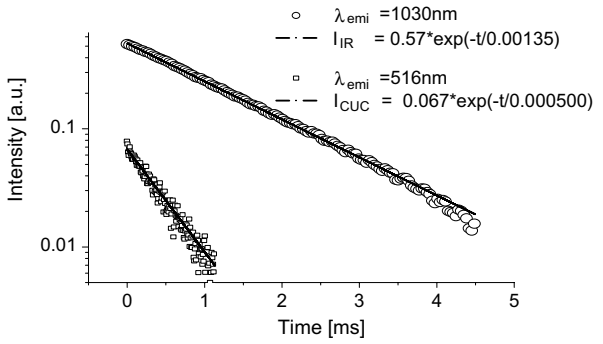

Fig. 5. Measured time decays of the IR and Cooperative upconversion (CUC) emissions from Yb^{3+} ions in NCYAG:Yb (5%). The pump wavelength was 940 nm.

are exponential and there is no observable rise time for the CUC emission decay. It is well known that for CUC if $I_{IR} \propto N_e \propto \exp(-t/\tau_{IR})$, then $I_{CUC} \propto N_e^2 \propto \exp \times (-2t/\tau_{IR})$, where N_e is the population of excited Yb^{3+} ions. We can observe that the measured life times for the IR and CUC emission agree well with the above sentence, since the CUC life time is almost half of the IR life time. The fact that both decays are exponential indicates that there is no sensible effect on these decays due to the deleterious upconversion emission from the Er^{3+} impurities. Than is consistent with the fact that the Er^{3+} ion concentration is expected to be in the order of traces.

The 1.35 ms luminescence decay time of the IR emission of the $^2F_{5/2}$ state for the NCYAG:Yb (5%) agrees very well with the reported value of 1.325 ms for bulk monocrystalline YAG:Yb (5%) [18,22]. These larger values are expected since YAG:Yb^{3+} is expected to present radiation trapping [23]. The difference between the NCYAG and Bulk YAG can be explained in terms of the model proposed by Meltzer et al. [24], where the effective life time of an emitting ion inside a nanocrystalline compound is lager than the life time of the same ion in a bulk host of the same compound. That elongation of the life time increases as the size of the nanoparticles decreases. The relationship among the bulk life time, τ_B, and that for the nanocrystalline host, τ_{NC}, derived from Eq. (1) in Ref. [24] by assuming the surrounding medium is air, is given by

$$\tau_{NC} = \tau_B \left(\frac{[(n^2+2)/3]^2 n}{[([nx+1-x)]^2+2)/3]^2 (nx+1-x)} \right), \qquad (3)$$

where n is the index of refraction of the bulk compound, and x is the filling factor that indicates the fraction of space occupied for the nanoparticles respect to the particle for which its size is that that the life time is equal to the bulk life time. For YAG $n = 1.82$, and by using the measured and reported life times at 1032 nm in Eq. (2), an estimation of the filling factor for our NCYAG:Yb (5%) samples turns to be of about

$x = 0.962$. Such a value indicates that for nanocrystals with an average size above 97.9 nm (=96 nm/x) there will be no observable differences in the life time from the bulk measurements. That also indicates that the NCYAG:Yb (5%) having a size of 96 nm are in the limit to be considered as nanoparticles that present confinement effects. It is also worth to notice that the 96 nm size is also in the limit of the definition for a particle to be considered as a nanoparticle, 100 nm. By introducing in Eq. (2) the estimated x value, $n = 1.846$ (at 516 nm), and the measured life time for the CUC emission (0.5 ms), an estimation of the life time for the CUC emission in bulk YAG:Yb (5%) turns to be 0.47015 ms. That value is in agreement with the value obtained for Malinowski for 24 μm thick planar Waveguides of YAG [5]. These results confirm that the size of 96 nm for the NCYAG:Yb (5%) samples is enough to start to observe confinement effects.

3. Conclusions

Enhanced cooperative absorption and upconversion emission of Yb^{3+} pairs in nanocrystalline YAG was observed. The nanocrystallites synthesized by a modified sol–gel method have an average size of 96 nm. The estimated concentration normalized ratio of maximum visible absorption to maximum IR absorption emission of $7.55 \times 10^{-22}\,cm^3$ is about four orders of magnitude higher than the highest value reported before. Strong cooperative upconversion emission is observed under IR pump at 940 nm. It is suggested that the enhanced cooperative processes are due to strong first neighbors interactions among RE ions. These strong interactions are promoted as a result of lattice distortion of superficial lattice cells, due to the nanosized character of NCYAG:Yb (5%), and the diffusion of RE ions to the surface of the nanocrystallites. The results are an increased relative concentration of RE ions near the nanocrystallite surface, and reduced minimum distances among RE ions near the surface of the nanocrystallite. Also life time measurements confirm that confinement effects are observed due to the 96 nm size of the nanophosphors. Further work is in progress to investigate the effects of the nanocrystallite size on the cooperative absorption and emission processes, as well on the effective life time of both IR and CUC emissions.

Acknowledgement

This work was partially supported by CONACyT, México, through grants 43168-F and G34629-E.

References

[1] P. Gerner, S. Heer, C. Reinhard, R. Valiente, O.S. Wenger, H.U. Güdel, Chimia 55 (12) (2001) 1021.
[2] S.M. Redmond, S.C. Rand, Opt. Lett. 28 (3) (2003) 173.
[3] M.J.V. Bell, W.G. Quirino, S.L. Oliveira, D.F. de Sousa, L.A.O. Nunes, J. Phys.: Condens. Matter. 15 (2003) 4877.
[4] V.V. Ovsyankin, P.P. Feofilov, Sov. Phys. JEPT Lett. 4 (1966) 317.
[5] M. Malinowski, M. Kaczkan, R. Piramidowicz, Z. Frukacz, J. Sarnecki, J. Lumin. 94–95 (2001) 29.
[6] G.S. Maciel, A. Biswas, R. Kapoor, P.N. Prasad, Appl. Phys. Lett. 76 (15) (2000) 1978.
[7] M.A. Noginov, G.B. Loutts, C.S. Steward, B.D. Lucas, D. Fider, V. Peters, E. Mix, G. Huber, J. Lumin. 96 (2002) 129.
[8] E. Montoya, L.E. Bausá, B. Schaudel, P. Goldner, J. Chem. Phys. 114 (7) (2001) 3200.
[9] E. Nazakawa, S. Shionaya, Phys. Rev. Lett. 25 (1970) 1710.
[10] F. Varsanyi, G.H. Dieke, Phys. Rev. Lett. 7 (1961) 442.
[11] J. Lu, T. Murai, K. Takaichi, T. Uematsu, M. Prabhu, J. Xu, K. Ueda, H. Yagi, T. Yanagitani, A.A. Kaminskii, A. Kudryashov, Appl. Phys. Lett. 78 (2000) 3586.
[12] J.F. Bisson, Y. Feng, A. Shirakawa, H. Yoneda, J. Lu, H. Yagi, T. Yanagitani, K. Ueda, Jpn. J. Appl. Phys. 42 (2003) L1025.
[13] J. Lu, K. Ueda, H. Yagi, T. Yanagitani, Y. Akiyama, A.A. Kaminskii, J. Alloys Comput. 340 (2002) 220.
[14] J. Lu, K. Takaichi, T. Uematsu, A. Shirakawa, M. Musha, K. Ueda, H. Yagi, T. Yanagitani, A.A. Kaminskii, Jpn. J. Appl. Phys. 41 (2002) L1373.
[15] J. Kong, D.Y. Tang, J. Lu, K. Ueda, H. Yagi, T. Yanagitani, Opt. Lett. 29 (11) (2004) 1212.
[16] E. De la Rosa, L.A. Díaz-Torres, P. Salas, A. Arredondo, J.A. Montoya, C. Angeles, R.A. Rodríguez, Low temperature synthesis and structural characterization of nanocrystalline YAG prepared by a modified sol–gel method, Opt. Mat., in press.
[17] C. Sanchez-Valle, I. Daniel, B. Reynard, R. Abraham, C. Goutaudier, J. Appl. Phys. 92 (8) (2002) 4349.
[18] J. Dong, M. Bass, Y. Mao, P. Deng, F. Gan, JOSA B 20 (9) (2003) 1975.
[19] R.A. Buchanan, K.A. Wickersheim, J.J. Pearson, G.F. Herrmann, Phys. Rev. 159 (2) (1967) 245.
[20] W.F. Krupke, IEEE J. Selected Topics QE 6 (2000) 1287.
[21] F.S. De Vicente, A.C. De Castro, M.F. De Souza, M. Siu Li, Thin Solid Films 418 (2002) 222.
[22] X. Xu, Z. Zhao, P. Song, G. Zhou, J. Xu, P. Deng, JOSA B 21 (3) (2004) 543.
[23] D.S. Sumida, T.Y. Fan, Opt. Lett. 19 (1994) 1343.
[24] R.S. Meltzer, S.P. Feofilov, B. Tissue, H.B. Yuan, Phys. Rev. B 60 (20) (1999) 14012.